ARTICLE

DOI: 10.1002/zaac.201200052

Cytotoxic, DNA Interaction, SOD Mimic, and Antimicrobial Activities of Square Pyramidal Copper(II) Complexes

Mohan N. Patel,*[a] Chintan R. Patel,[a] and Hardik N. Joshi[a]

Keywords: NS donor ligand; Ciprofloxacin; Antibacterial activity; DNA interaction; Cytotoxicity; Copper

Abstract. The copper(II) complexes with NS donor ligand and ciprofloxacin were synthesized. The synthesized complexes were characterized by physicochemical parameters like elemental and thermal analysis, electronic, FT-IR, and LC-MS spectroscopy. The complexes were tested for their antibacterial activity against two Gram(+ve) i.e. *Staphylococcus aureus*, *Bacillus subtilis* and three Gram(–ve) i.e., *Serratia marcescens*, *Pseudomonas aeruginosa, Escherichia coli* bacteria in terms of MIC (μM) and the results were compared with the parent drug. Viscosity measurement and absorption titration were employed to determine the mode of binding of complexes with DNA. DNA cleavage activity was carried out by gel electrophoresis experiment using supercoiled form of pUC19 DNA. The complexes were screened for their SOD mimic activity in terms of IC_{50} value. The complexes were also checked for their cytotoxicity using brine shrimp assay method.

1 Introduction

Quinolones are synthetic antibacterial agents widely used in clinical practice. Ciprofloxacin [1-cyclopropyl-6-fluoro-1,4-dihydro-4-oxo-7-(1-piperazinyl)-3-quinoline carboxylic acid] is a member of this large family and is used for the treatment of certain diseases caused by various Gram(-ve) and some Gram(+ve) positive microorganisms.[1] Fluoroquinolone drugs act intravenously by inhibiting topoisomerase II (DNA gyrase) or topoisomerase.[2] It is generally accepted that the quinolone target the bacterial enzyme gyrase–DNA complex, which is responsible for the supercoiling of bacterial DNA.[3] Many transition metal complexes are used as potential probes of nucleic acid structure and for potential application as drugs.[4] The complexes of vanadium(IV), copper(II), magnesium(II), uranium(VI), manganese(II), iron(III), cobalt(II), nickel(II), molybdenum(II), and europium(III) with ciprofloxacin have been synthesized and explored for their biological activities because of its biological relevance.[5–12]

Superoxide anion ($O_2^{\cdot-}$) is essential for the biological defence system against the invasion of bacteria and viruses, but it is also known for its pathogeneses of many disease processes, including inflammatory damage and DNA damage and aging.[13,14] Use of synthetic SOD mimic for pharmaceutical purposes are problematic due to difficulties associated with the systematic infection of protein, i.e. the circulation lifetime, cell impermeability, immunogenicity, tissue, antigenicity, and high costs. To avoid such limitations, there has been a considerable interest in developing synthetic SOD mimics that have low molecular weight, biological stability, membrane permeability, nontoxic and low cost.[15,16]

In continuation of our previous work,[17] herein we report ternary Cu^{II} complexes with ciprofloxacin and neutral bidentate ligands with NS donor atom. In-vitro antimicrobial activity was performed against two Gram(+ve) and three Gram(–ve) microorganisms using double dilution method. The synthesized complexes were checked for their DNA interactions using absorption titration, viscosity measurement, and gel electrophoresis. The SOD mimic behavior of the complexes was checked under non-enzymatic condition. The synthesized complexes were also checked for their cytotoxic effect using brine shrimp lethality bioassay.

2 Result and Discussion

2.1 Synthesis and Characterization of Complexes

The ternary Cu^{II} complexes were prepared by the reaction of Cu^{II} chloride with ciprofloxacin and different bidentate NS donor ligands (A^1–A^6) in a ratio of 1:1:1 refluxed for 3 h on water bath maintaining pH = 6.8 of the reaction mixture. A fine amorphous product obtained was washed with chloroform and dried in vacuum. The synthesized complexes were characterized by FT-IR, UV/Vis spectroscopy, magnetic measurement, thermogravimetric analysis and LC-MS techniques. All the complexes are insoluble in water, ethanol, methanol, dichloromethane, chloroform, acetonitrile, hexane, and DMF, whereas they are soluble in DMSO, so it is difficult to grow crystals for X-ray diffraction analysis. All the physicochemical parameters data are in good agreement and suggest the square pyramidal arrangement around the central metal ion. The pro-

* Prof. Dr. M. N. Patel
E-Mail: jeenen@gmail.com
[a] Department of Chemistry
Sardar Patel University
Vallabh Vidyanagar-388 120
Gujarat, India

Supporting information for this article is available on the WWW under **http://dx.doi.org/10.1002/zaac.201200052** or from the author.

 WILEY ONLINE LIBRARY © 2012 WILEY-VCH Verlag GmbH & Co. KGaA, Weinheim

Zeitschrift für anorganische und allgemeine Chemie ZAAC Journal of Inorganic and General Chemistry

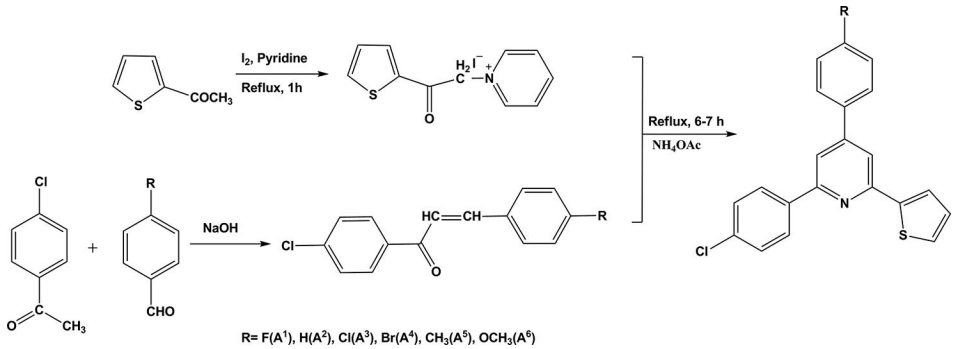

Scheme 1. General synthesis of ligands and proposed structures.

posed structure and general synthesis of ligands and complexes are shown in Scheme 1 and Scheme 2, respectively.

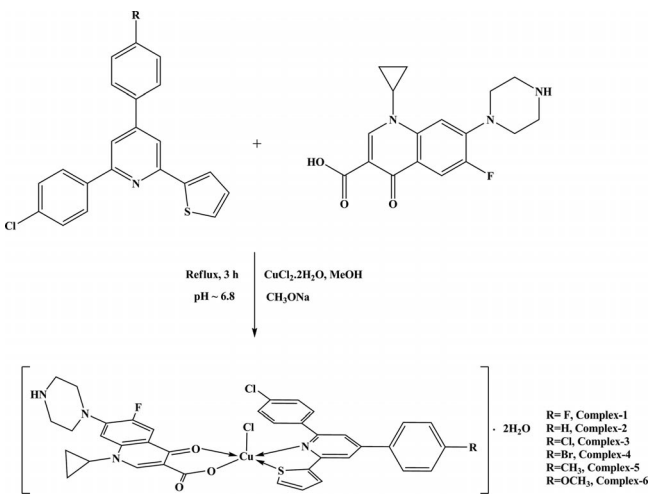

Scheme 2. Proposed structures and general synthesis of complexes.

2.1.1 Spectrophotometric Titration

The amount of copper was determined by spectrophotometric titration technique. Sample solutions were prepared by decomposing organic matter of complex with acid mixture and making it to total volume of 20 mL with double distilled water. Ten different sets of solutions were prepared by taking a fixed amount of complex solution (2 mL), 2 mL acetate buffer solution and varying aliquots of 0.0005 M EDTA and making it to total volume of 10 mL with double distilled water. Absorbance was measured at 745 nm using buffer as a reference. The amount of copper was determined using the plot of absorbance against different volume of EDTA used during the spectrophotometric titration.[18,19] The calculated results from the equivalent endpoint reveal the metallic content of the complexes (Table 1 and Supporting Information).

2.1.2 IR Spectroscopy

In the IR spectrum of ciprofloxacin the valence vibration of the carboxylic stretch $\nu(C{=}O)_{carb}$ is found at 1708 cm^{-1} and the pyridone stretch $\nu(C{=}O)_{p}$ at 1624 cm^{-1}. The characterization of quinolones metal complexes can be achieved by studying the most typical vibrations that are characteristic of the coordination type of quinolones.

On complexation, these bands appear between 1575–1584 and 1352–1360 cm^{-1}. The frequency of separation $\Delta\nu = \nu(COO)_{as} - \nu(COO)_{s}$ in investigated complexes is ca. 200 cm^{-1}, suggesting the unidentate nature for the carboxylato group.[20,21] A sharp band at 3520 cm^{-1} due to stretching vibration of free hydroxyl in quinolone moiety is completely disappeared in the spectra of complexes.[22] The band at 1624 cm^{-1} responsible for $\nu(C{=}O)_{p}$ in ciprofloxacin is observed between 1622–1632 cm^{-1} in case of complexes.[12,23] These data are further supported by the weak bands observed at 575–540, 525–490, and 485–440 cm^{-1}, which are assigned to $\nu(M{-}O)$, $\nu(M{-}N)$,[24,25] and $\nu(M{-}S)$[26] vibrations, respectively (Table 2).

2.1.3 Electronic Spectra and Magnetic Data

A visible emission spectra of the copper(II) complexes i.e. d^9 system were recorded in DMSO. The complexes exhibited the only broad peak at λ_{max} = ca. 660 nm, which was attributed to d–d transition, in which the Cu^{II} atom was in a distorted square pyramidal environment.[27,28] The possibility of trigonal bipyrimidal arrangement at the central metal atom was ruled out because a peak of λ_{max} greater than 800 nm along with a shoulder at ca. 660 nm was not observed in the case of synthesized complexes.[29,30]

The magnetic moments measurement for any arrangement in copper(II) complexes generally results in the range 1.76–1.88 BM, which is very close to the spin-only value i.e. 1.73 BM. The observed values in our case were very close to the spin-only values (Table 1) for single unpaired electrons and confirm the copper in +2 state with d^9 configuration ($t_{2g}^6\ e_g^3$).[31,32]

 © 2012 WILEY-VCH Verlag GmbH & Co. KGaA, Weinheim

Table 1. Theoretical and found copper content for the synthesized complexes **1–6**.

	1	**2**	**3**	**4**	**5**	**6**
Cu experimental /%	7.73	8.09	7.49	7.26	8.01	7.66
Cu theoretically /%	7.64	7.81	7.5	7.12	7.68	7.54

Table 2. Characteristic absorptions bands of IR spectra of the complexes and CPFH /cm^{-1}.

	ν(C=O) pyridone	$\nu(COO)_{as}$	$\nu(COO)_s$	Δν	ν(*M*–O)	ν(*M*–N)	ν(*M*–S)
CPFH	1624	1708[a]	–	–	–	–	–
$[Cu(CPF)A^1Cl]\cdot 2H_2O$ (**1**)	1632	1584	1356	228	575	490	470
$[Cu(CPF)A^2Cl]\cdot 2H_2O$ (**2**)	1627	1577	1360	217	560	520	485
$[Cu(CPF)A^3Cl]\cdot 2H_2O$ (**3**)	1622	1575	1352	223	545	515	450
$[Cu(CPF)A^4Cl]\cdot 2H_2O$ (**4**)	1625	1577	1354	223	570	505	465
$[Cu(CPF)A^5Cl]\cdot 2H_2O$ (**5**)	1630	1576	1355	221	565	510	455
$[Cu(CPF)A^6Cl]\cdot 2H_2O$ (**6**)	1629	1578	1358	220	540	525	440

a) As ν(COOH).

2.1.4 LC-MS Spectra Analysis

Material 2 (Supporting Information) shows the mass spectrum of complex $[Cu(CPF)(A^1)Cl]\cdot 2H_2O$. The mass spectrum of complex **1** (Figure 1, mass fragmentation pattern of complex **1**) shows molecular ion peak [M^+] at 795.18 *m/z* and [M + 2] at 797.19 *m/z*. Peaks at 464.85 *m/z* and 466.55 *m/z* are due to ligand attached with copper and one chlorine atom. The peaks at 429.40 *m/z* and 431.33 *m/z* correspond to the removal of coordinated chlorine atom from the central metal ion. The peak at 429.33 *m/z* is due to ciprofloxacin attached to copper(II) including coordinated chlorine atom. The peaks at 365.85 *m/z* and 367.75 *m/z* are due to the loss of copper from neutral bidentate ligand. The peak at 331.15 *m/z* corresponds to ciprofloxacin moiety. The peaks at 283.10 *m/z* and 285.15 *m/z* are due to fragmentation of bidentate ligand and the peak at 247.14 *m/z* corresponds to loss of piperidine moiety from ciprofloxacin. The peak at 203.21 *m/z* is due to the loss of the COOH group from fragment of ciprofloxacin.

2.1.5 Thermogravimetric Analysis

TGA data indicate that complex **1** decomposes in three steps.[33] From the characteristic thermogravimetric curve (mass loss in % to temperature in °C), it is clear that loss occurring during the first step i.e. 40–120 °C (found ca. 4.5%, theoretical 4.33%) corresponds to loosely bonded two molecules of water of crystallization. The mass lose (found ca. 44%, theoretical 44.13%) during the second step (200–

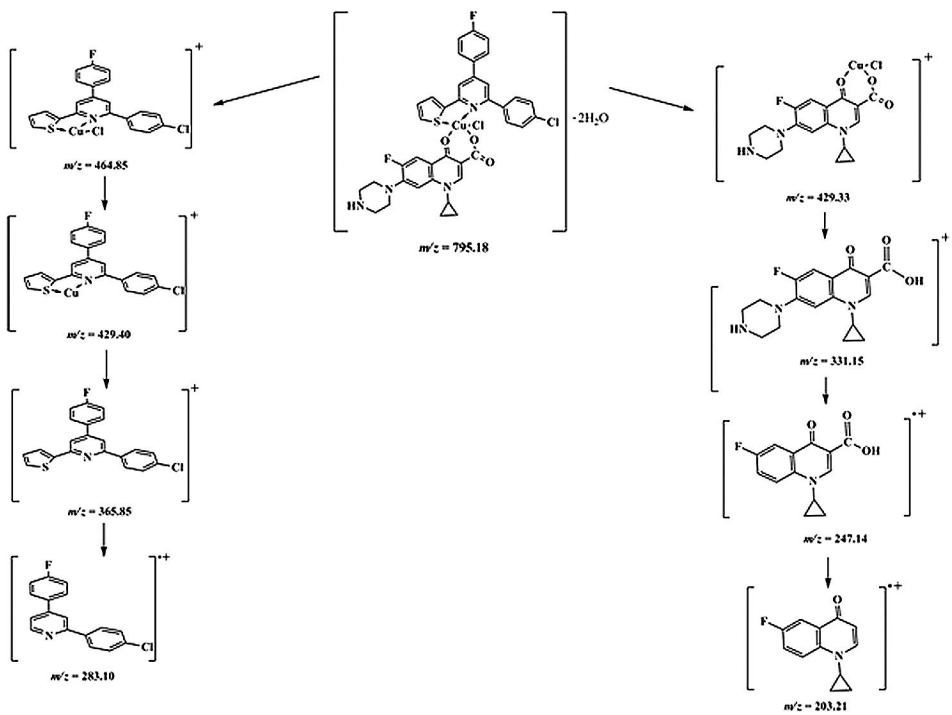

Figure 1. Proposed mass fragmentation pattern of $[Cu(CPF)A^1Cl]\cdot 2H_2O$ (**1**).

 © 2012 WILEY-VCH Verlag GmbH & Co. KGaA, Weinheim

Zeitschrift für anorganische und allgemeine Chemie ZAAC Journal of Inorganic and General Chemistry

Table 3. Antimicrobial activities of CPFH, copper(II) salt, and complexes **1–6** in terms of Minimum Inhibitory Concentration (MIC) /μM.

	Gram positive *S.aureus*	*B.subtilis*	Gram negative *S.marcescens*	*P .aeruginosa*	*E. coli*
$CuCl_2{\cdot}2H_2O$	2698.0	2815.0	2756.0	2404.0	3402.0
CPFH	1.52	1.04	1.52	1.32	1.36
$[Cu(CPF)A^1Cl]{\cdot}2H_2O$ (**1**)	0.72	0.20	0.40	0.82	0.80
$[Cu(CPF)A^2Cl]{\cdot}2H_2O$ (**2**)	0.96	0.50	0.80	1.15	1.10
$[Cu(CPF)A^3Cl]{\cdot}2H_2O$ (**3**)	0.75	0.25	0.45	0.90	0.85
$[Cu(CPF)A^4Cl]{\cdot}2H_2O$ (**4**)	0.80	0.40	0.48	1.10	0.94
$[Cu(CPF)A^5Cl]{\cdot}2H_2O$ (**5**)	1.28	0.70	0.95	1.25	1.30
$[Cu(CPF)A^6Cl]{\cdot}2H_2O$ (**6**)	1.50	0.96	1.60	1.32	1.35

470 °C) corresponds to loss of ciprofloxacin and chlorine. In the third step mass loss (found ca. 44.10%, theoretical 44.01%) corresponds to decomposition of neutral bidentate ligand (470–835 °C) occurs, leaving behind metal oxide as residue (found ca. 9.70%, theoretical 9.57%) (see Supporting Information).

2.2 Biological Evaluation

2.2.1 In-vitro Antimicrobial Screening

Synthesized complexes, ciprofloxacin, and metal salt were checked for their in-vitro antibacterial activity in terms of minimum inhibitory concentration (MIC) against bacterial strain such as *E. coli*, *P. aeruginosa*, *S. aureus*, *B. Subtilis*, and *S. marcescens* (Table 3).

Following conclusion is drawn from the antibacterial data:

(1) *S. aureus*: Complexes **1**, **2**, **3**, and **4** are more active compared to other complexes and ciprofloxacin.

(2) *B. subtilis*: All the complexes show better activity compare to ciprofloxacin.

(3) *S. marcescens*: Except complex **6** all other complexes are more potent than ciprofloxacin.

(4) *P. aeruginosa*: Complexes **1**, **3** and **4** are more active than other complexes and ciprofloxacin.

(5) *E. coli*: Complexes **1**, **2**, **3**, and **4** are more active compared to other complexes and ciprofloxacin.

The good antimicrobial activity is observed may be studied under following five principles.[34]

(1) The chelate effect, i.e. ligands that are bound to metal ions in a bidentate fashion, such as the quinolones and phenanthroline, bipyridine, or bipyridylamine show higher antimicrobial efficiency towards complexes with nitrogen donor ligands.

(2) Nature of the ligands.

(3) The total charge of the complex; generally the antimicrobial efficiency decreases in the order cationic > neutral > anionic complex.

(4) The nature of the ion neutralizing the ionic complex.

(5) The nuclearity of the central metal atom in the complex; dinuclear centers are usually more active than mononuclear ones.

Thus, first two factors may be considered for increase in the activity i.e. chelate effect.

In addition, our study regarding bactericidal activity in terms of $CFU{\cdot}mL^{-1}$ of above metal complexes against same microorganisms reveals that, decrease in number of colonies with increasing the concentration of complexes. The results are shown in Figure 2 for all the complexes against *B. subtilis* (see Supporting Information). The number of colonies counted in this technique was 30–300. From the minimum inhibitory concentration (MIC) values and colony forming units (CFU), one can conclude that complex **1** showed more potency against all the five microorganisms than other complexes.

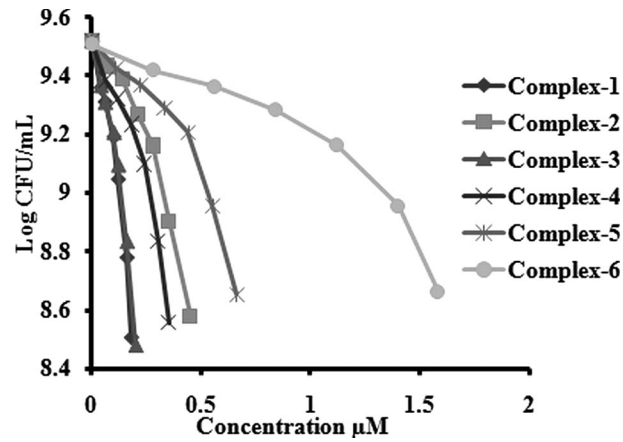

Figure 2. Plot of log(CFU/mL) versus concentration (μg/mL) for all complexes against *B. subtilis*.

2.2.2 DNA Binding Study by Absorption Titration

DNA can provide three distinctive binding sites for the quinolone complexes; namely, groove binding, binding to phosphate groups, and intercalation. This behavior is of great importance with regard to the biological role of fluoroquinolone antibiotics in the human body.[35] When complex interacts with DNA by intercalative mode it results in hypochromism and red shift, as intercalative mode involving a strong stacking interaction between the aromatic chromophore and the base pairs of DNA. The magnitude of the hypochromism and red shift are commonly found to depend on the strength of the intercalative interaction.[36] It is a general observation that the binding of intercalative molecules to DNA is accompanied by a red shift and hypochromism in the absorption spectra.[37] The extent of spectral change is related to the strength of binding. The absorption spectra of the complex in absence and presence of DNA is illustrated in Figure 3. In order to compare quantitatively the binding strength of the complexes, the intrinsic binding constant K_b was obtained by monitoring the changes in

 © 2012 WILEY-VCH Verlag GmbH & Co. KGaA, Weinheim

absorbance for complexes with increasing concentration of DNA. This is lower than K_b value of classical intercalator ethidium bromide but higher than reported Cu^{II} complexes[38–41] and different metal quinolone complexes.[42,43] From the K_b value and red shift, it is clear that the complexes bind by intercalation mode and complex **1** has the highest binding ability (Table 4).

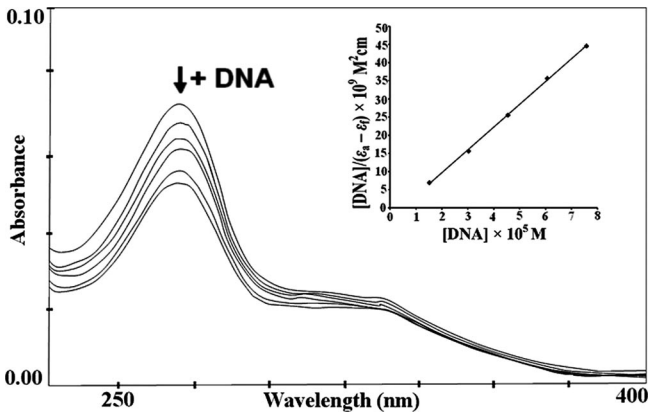

Figure 3. Electronic absorption spectra of $[Cu(CPF)A^1Cl]\cdot 2H_2O$ (**1**) in phosphate buffer (Na_2HPO_4/NaH_2PO_4, pH 7.2) in the absence and presence of increasing amount of DNA. The [Cu] complex = 10 μM; [DNA] = 0–150 μM. The incubation period is 10 min. at room temperature, Inset: Plot of $[DNA]/(\varepsilon_a-\varepsilon_f)$ versus [DNA]. Arrow shows the absorbance change upon increasing DNA concentrations.

Table 4. Binding constant (K_b), IC_{50}, and LC_{50} values of synthesized complexes.

	K_b /M^{-1}	IC_{50} /μM	LC_{50} /μM
$[Cu(CPF)A^1Cl]\cdot 2H_2O$ (**1**)	3.17×10^5	0.59	6.02
$[Cu(CPF)A^2Cl]\cdot 2H_2O$ (**2**)	1.36×10^5	0.97	10.30
$[Cu(CPF)A^3Cl]\cdot 2H_2O$ (**3**)	2.42×10^5	0.68	7.96
$[Cu(CPF)A^4Cl]\cdot 2H_2O$ (**4**)	2.16×10^5	0.83	10.02
$[Cu(CPF)A^5Cl]\cdot 2H_2O$ (**5**)	0.88×10^5	1.03	16.73
$[Cu(CPF)A^6Cl]\cdot 2H_2O$ (**6**)	0.49×10^5	1.11	19.28

2.2.3 DNA Binding Study by Viscosity Measurement

Optical photophysical probes provide necessary, but insufficient clues to support binding mode. In absence of crystallographic structural data viscosity measurement, sensitive to length change is regarded as the least ambiguous and the most critical tests for determining binding mode in solution state.[44] A classical intercalation model usually resulted in lengthening the DNA helix, as base pairs were separated to accommodate the binding ligand leading to the increase of DNA viscosity.[41] Intercalation of a molecule into DNA could result in lengthening, unwinding, and stiffening of the helix and is usually accompanied by increase in solution viscosity.[45] Figure 4 shows the binding ability of ethidium bromide, complexes, and ciprofloxacin. In our case increase in viscosity was observed, which was less compared to classical intercalator ethidium bromide and more compared to ciprofloxacin. Hence, complexes bind to DNA by classical intercalation mode and complex **1** interacts more strongly compared to the other complexes.

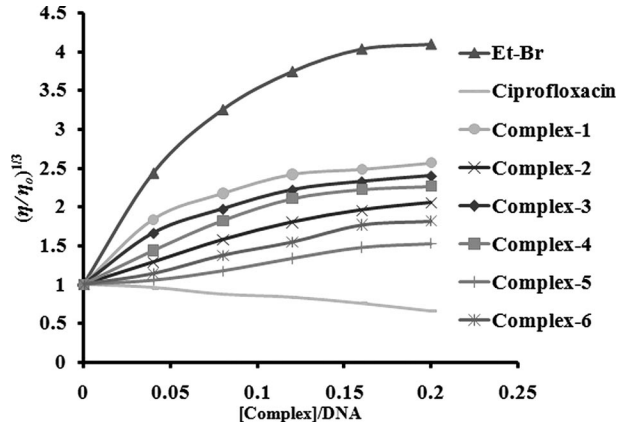

Figure 4. Effects of increasing amounts of EtBr, CPFH and complexes on the relative viscosity of herring sperm DNA at 37 ± 0.1 °C.

2.2.4 DNA Cleavage Study by Gel Electrophoresis

There has been considerable interest in DNA cleavage reactions that are activated by transition metal complexes.[45,46] Agarose gel electrophoresis was used as a base for monitoring plasmid DNA cleavage reaction. When plasmid DNA is subjected to electrophoresis, relatively fast migration is observed for the intact supercoil form (Form I). The scission on one strand (nicking) will relax supercoil to generate a slower-moving open circular (Form II), and if both strands are cleaved, a linear (Form III) that migrates between Form I and Form II will be generated.[47] The data of the cleavage study obtained from Figure 5 are presented in Table 5, which show that synthesized complexes have better cleavage ability than metal salt and ciprofloxacin.

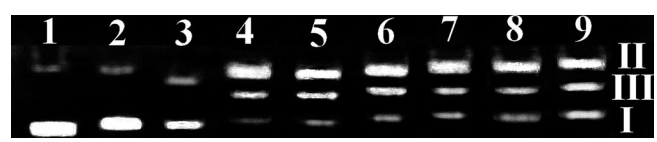

Figure 5. Photogenic view of cleavage of pUC19 DNA (300 μg/mL) with series of copper(II) complexes (200 μM) using 1% agarose gel containing 0.5 μg/mL ethidium bromide. All reactions were incubated in TE buffer (pH 8) in a final volume of 15 μL, for 24 h. at 37 °C. Lane 1, DNA control; Lane 2, $CuCl_2\cdot 2H_2O$; Lane 3, Ciprofloxacin; Lane 4, $[Cu(CPF)A^1Cl]\cdot 2H_2O$ (**1**); Lane 5, $[Cu(CPF)A^2Cl]\cdot 2H_2O$ (**2**); Lane 6, $[Cu(CPF)A^3Cl]\cdot 2H_2O$ (**3**); Lane 7, $[Cu(CPF)A^1Cl]\cdot 2H_2O$ (**4**); Lane 8, $[Cu(CPF)A^5Cl]\cdot 2H_2O$ (**5**); Lane 9, $[Cu(CPF)A^6Cl]\cdot 2H_2O$ (**6**).

2.2.5 SOD-like Activity

The system used as a source of superoxide radical generator in order to check SOD like activity for the synthesized complexes was the NBT/NADH/PMS system. The percent inhibition of formazan formation at various concentrations of complexes as a function of time was determined by measuring the absorbance at 560 nm and plotted to have a straight line obeying equation Y = mX + C (Figure 6); with increase in concentration of tested complexes deterioration in slope (m) was ob-

 © 2012 WILEY-VCH Verlag GmbH & Co. KGaA, Weinheim

Zeitschrift für anorganische und allgemeine Chemie ZAAC Journal of Inorganic and General Chemistry

Table 5. Complex mediated DNA cleavage data by gel electrophoresis.

Lane No.	Compound	Form I	Form II	Form III	Cleavage /%
		SC	OC	L	
1	Control	82	18	–	–
2	$CuCl_2{\cdot}2H_2O$	76	24	–	7.31
3	Ciprofloxacin	61	39	–	25.60
4	$[Cu(CPF)A^1Cl]{\cdot}2H_2O$ (**1**)	10	60	30	87.80
5	$[Cu(CPF)A^2Cl]{\cdot}2H_2O$ (**2**)	20	51	29	73.17
6	$[Cu(CPF)A^3Cl]{\cdot}2H_2O$ (**3**)	18	52	31	78.04
7	$[Cu(CPF)A^4Cl]{\cdot}2H_2O$ (**4**)	20	54	26	75.60
8	$[Cu(CPF)A^5Cl]{\cdot}2H_2O$ (**5**)	24	49	27	70.73
9	$[Cu(CPF)A^6Cl]{\cdot}2H_2O$ (**6**)	29	41	30	64.63

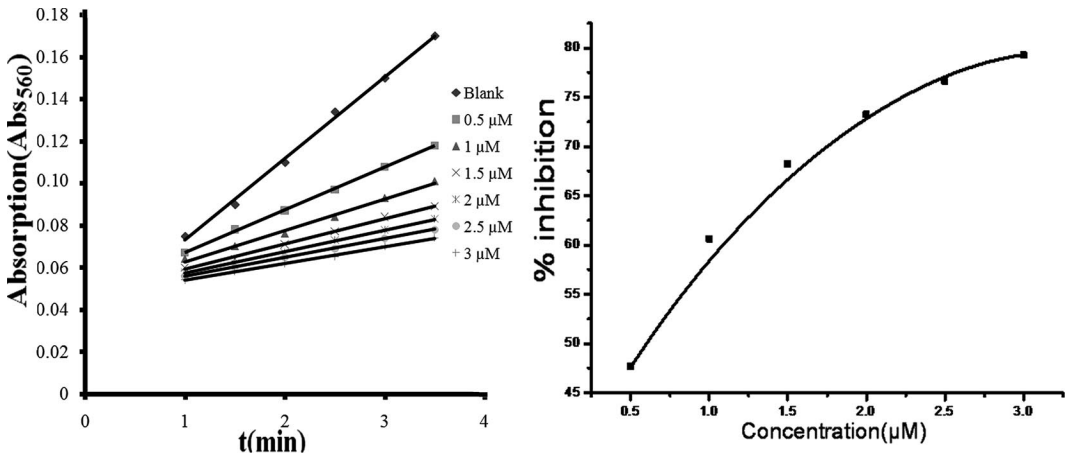

Figure 6. Plot of absorbance (Abs560) as a function of time (t) to determine % inhibition of formazan formation at various concentrations of complex **1** (0.5 μm to 3 μm) as function of time and the plot of percentage of inhibiting NBT reduction with an increase in the concentration of complex **1**.

served. Percent inhibition of the reduction of nitro blue tetrazolium (NBT) was plotted against the concentration of the complex **1** to obtain IC_{50} values (Figure 6). Complexes exhibit SOD-like activity at biological pH with their IC_{50} values ranging from 0.59 to 1.11 μM. The superoxide scavenging data are presented in Table 4. The best IC_{50} value among synthesized complexes is observed for complex **1**. The higher IC_{50} can only be accredited to the vacant coordination site facilitating the binding of superoxide anion, electrons of aromatic ligands that stabilize $Cu–O_2^-$ interaction and not only to the partial dissociation of complexes in solution. The mechanism for scavenging of superoxide radical moves forward via unstable octahedral adduct under the influence of Jahn-Teller effect,[48,49] and there is a possibility of rapid inter-conversion between Cu^{II} and Cu^{I} via electron transfer between copper and reactive oxygen radical anion following the principle of electroneutrality.[50]

2.2.6 Cytotoxic Activity - Brine Shrimp Lethality Bioassay

From the data, percent of mortality was calculated and plotted against log dose (see Supporting Information). LC_{50} values of test complexes observed after 24 h are shown in Table 4. From the results, it is found that the complexes show considerable cytotoxicity in the brine shrimp (*Artemia cysts*) lethality bioassay. And among all the complexes, complex **1** shows maximum activity.

3 Conclusions

Data of magnetic behavior and electronic spectral measurement points towards the d^9 system with distorted square pyramidal arrangement. The electronic absorption data are in good accordance with viscosity titration curves. The reason behind increase in potency of drug is due to its coordination with metal ion. The data from SOD mimic activity suggests that, the higher activity is due to vacant coordination site at the central metal ion. The DNA cleavage study of pUC19 shows that all complexes have higher cleavage ability than metal salt and drug. Such a trend in result shows that the DNA interaction ability, free radical scavenging ability, antimicrobial activity, and cytotoxicity of the synthesized complexes can be controlled by the substituent of the intercalative ligand. It also concluded from the results that as the electron withdrawing ability of substituent (F, Cl, Br) on the intercalative ligand increases, the DNA interaction ability, free radical scavenging ability and antimicrobial activity increases and vice-versa for the electron releasing substituent (CH_3, OCH_3).

 © 2012 WILEY-VCH Verlag GmbH & Co. KGaA, Weinheim

4. Experimental Section

4.1 Materials and Reagents

All solvents, chemicals, and reagents used were of analytical reagent grade and were used as such; double distilled water was used throughout. Ciprofloxacin (CPFH) was purchased from Bayer AG (Wuppertal, Germany). Cupric chloride was purchased from E. Merck (India) Ltd. Mumbai. Benzaldehyde, 4-fluoro benzaldehyde, 4-chloro benzaldehyde, 4-bromo benzaldehyde, 4-methyl benzaldehyde, 4-methoxy benzaldehyde, and 2-acetyl thiophene were purchased from Spectrochem Pvt. Ltd. Mumbai (India). Luria Broth, agarose, ethidium bromide, TAE (tris-acetyl-EDTA), bromophenol blue, and xylene cyanol FF were purchased from Himedia, India. Nicotinamide adenine dinucleotide reduced (NADH), nitro blue tetrazolium (NBT) and phenazin methosulphate (PMS) were purchased from Loba Chemie Pvt. Ltd. Herring Sperm DNA was purchased from Sigma Chemical Co. (India).

4.2. Physical Measurements

Elemental analyses (C, H, and N) of the synthesized complexes were performed with a model 240 Perkin-Elmer elemental analyzer, Massachusetts (USA). Metallic content of the complex was determined after decomposing it under effect of acid mixture and titrating against EDTA solution volumetrically. Room temperature magnetic measurement for the complexes was made using Gouy magnetic balance. The Gouy tube was calibrated using mercury(II)tetrathiocyanatocobaltate(II) as the calibrant ($\chi_g = 16.44 \times 10^{-6}$ cgs units at 20 °C). The electronic spectra were recorded with a UV-160A UV-Vis spectrophotometer, Shimadzu, Kyoto (Japan). Infrared spectra were recorded with a FT-IR ABB Bomen MB-3000, (Canada) spectrophotometer as KBr pellets in the range 4000–400 cm^{-1}. MIC study was carried out by means of laminar air flow cabinet, Toshiba, Delhi, (India). The thermogram of complexes was recorded with a Mettler Toledo TGA/DSC 1 thermogravimetric analyzer. The LC-MS spectra were recorded with a Thermo mass spectrophotometer (USA). Photo quantization of the gel after electrophoresis was done using AlphaDigiDoc™ RT. Version V.4.0.0 PC–Image software, California (USA).

4.3. General Synthesis of Ligands

The ligands were prepared by a modified *Krönke* pyridine synthesis[51] using halo pyridinium salt of 2-acetyl thiophene, ammonium acetate, and different chalcone in methanol. The mixture was reflux for 6–7 h on a sand bath. The product was obtained by keeping the solution in an ice bath and purified by crystallization in *n*-hexane. Ligands were characterized by elemental analysis, ^1H and ^{13}C NMR spectroscopy (see Supporting Information).

4.4. General Synthesis of Complexes

A methanol solution of $CuCl_2 \cdot 2H_2O$ (1 mmol) was added to a methanol solution of neutral bidentate ligand (A^n) (1 mmol), followed by addition of previously prepared methanol solution of ciprofloxacin in presence of CH_3ONa (1 mmol). The pH of reaction mixture was adjusted at ca. 6.8 using dilute solution of CH_3ONa. The resulting solution was refluxed for 3 h. on a water bath, followed by concentrating it to half of its volume. A fine amorphous product obtained was washed with chloroform and dried in vacuo desiccators.

[Cu(CPF)A^1Cl]·$2H_2O$ (1): prepared by using 2-(4-chlorophenyl)-4-(4-fluorophenyl)-6-(thiophen-2-yl)pyridine (A^1) (1 mmol). Yield 53 %, m.p. >300 °C, μ_{eff}: 1.80 B.M. *m/z* = 795.18. $C_{38}H_{34}Cl_2CuF_2N_4O_5S$ (831.21): calcd. (found) C 54.91 (55.10); H 4.12 (4.01); N 6.74 (6.67); S 3.86 (3.92), Cu 7.64 (7.73) %. $\lambda_{max(solid)}$ = 676 nm, $\lambda_{max(solution)}$ = 656 nm, ε = 94.11 $M^{-1} \cdot cm^{-1}$ (1.02×10^{-3}M).

[Cu(CPF)A^2Cl]·$2H_2O$ (2): prepared by using 2-(4-chlorophenyl)-4-phenyl-6-(thiophen-2-yl)pyridine (A^2) (1 mmol). Yield 49 %, m.p. >300 °C, μ_{eff}: 1.84 B.M. *m/z* = 777.02. $C_{38}H_{35}Cl_2CuFN_4O_5S$ (813.22): calcd (found) C 56.12 (56.60); H 4.34 (4.45); N 6.89 (7.05); S 3.94 (4.05), Cu 7.81 (8.09) %. $\lambda_{max(solid)}$ = 680 nm, $\lambda_{max(solution)}$ = 670 nm, ε = 78.27 $M^{-1} \cdot cm^{-1}$ (5.75×10^{-4}M).

[Cu(CPF)A^3Cl]·$2H_2O$ (3): prepared by using 2,4-bis(4-chlorophenyl)-6-(thiophen-2-yl)pyridine (A^3) (1 mmol). Yield 65 %, m.p. >300 °C, μ_{eff}: 1.76 B.M. *m/z* = 811.47. $C_{38}H_{34}Cl_3CuFN_4O_5S$ (847.67): calcd (found) C 53.23 (53.29); H 4.04 (3.90); N 6.61 (6.47); S 3.78 (3.65), Cu 7.50 (7.49) %. $\lambda_{max(solid)}$ = 651 nm, $\lambda_{max(solution)}$ = 636 nm, ε = 100.77 $M^{-1} \cdot cm^{-1}$ (8.13×10^{-4}M).

[Cu(CPF)A^4Cl]·$2H_2O$ (4): prepared by using 4-(4-bromophenyl)-2-(4-chlorophenyl)-6-(thiophen-2-yl)pyridine (A^4) (1 mmol). Yield 46 %, m.p. >300 °C, μ_{eff}: 1.78 B.M. *m/z* = 856.04. $C_{38}H_{34}Cl_2CuBrFN_4O_5S$ (892.12): calcd (found) C 51.16 (51.20); H 3.84 (3.68); N 6.28 (6.30); S 3.59 (3.43), Cu 7.12 (7.26) %. $\lambda_{max(solid)}$ = 680 nm, $\lambda_{max(solution)}$ = 665 nm, ε = 76.38 $M^{-1} \cdot cm^{-1}$ (7.72×10^{-4}M).

[Cu(CPF)A^5Cl]·$2H_2O$ (5): prepared by using 2-(4-chlorophenyl)-6-(thiophen-2-yl)-4-p-tolylpyridine (A^5) (1 mmol). Yield 57 %, m.p. >300 °C, μ_{eff}: 1.88 B.M. *m/z* = 791.16. $C_{39}H_{37}Cl_2CuFN_4O_5S$ (827.25): calcd (found) C 56.62 (56.35); H 4.51 (4.42); N 6.77 (6.67); S 3.88 (3.82), Cu 7.68 (8.01) %. $\lambda_{max(solid)}$ = 685 nm, $\lambda_{max(solution)}$ = 675 nm, = 88.76 $M^{-1} \cdot cm^{-1}$ (8.33×10^{-4}M).

[Cu(CPF)A^6Cl]·$2H_2O$ (6): prepared by using 2-(4-chlorophenyl)-4-(4-methoxyphenyl)-6-(thiophen-2-yl)pyridine (A^6) (1 mmol) Yield 45 %, m.p. >300 °C, μ_{eff}: 1.77 B.M. *m/z* = 807.17. $C_{39}H_{37}Cl_2CuFN_4O_6S$ (843.25): calcd (found) C 55.55 (55.90); H 4.42 (4.30); N 6.64 (6.60); S 3.80 (3.75), Cu 7.54 (7.66) %. $\lambda_{max(solid)}$ = 665 nm, $\lambda_{max(solution)}$ = 650 nm, ε = 82.94 $M^{-1} \cdot cm^{-1}$ (9.40×10^{-4}M).

4.5 Biological Screening of Synthesized Complexes

4.5.1 In-vitro Antimicrobial Screening

The antibacterial activity of the complexes was studied against *E. coli* (MTCC-433), *P. aeruginosa* (MTCC-1688), *B. subtilis* (MTCC-7193), *S. aureus* (MTCC-3160) and *S. marcescens* (MTCC-7103). Screening was performed by determining the minimum inhibitory concentration (MIC) using Luria Broth (LB) as a medium. The complexes were dissolved in DMSO. Cultured for Gram(+ve) and Gram(–ve) were incubated at 37 °C. Control test with no active ingredient was also performed.[52] MIC was determined using two fold serial dilution in liquid media containing 0.2–3,500 μM variation of test complex concentration. A pre-culture of bacteria was grown in LB overnight at the optimal temperature of each species. Bacterial growth was monitored by measuring the turbidity of the culture after 18 h. If a certain concentration of a complex inhibits the bacterial growth, half the concentration of the complex was tested. This procedure was carried on to a concentration that bacteria grow normally. The lowest concentration that inhibits the bacterial growth was determined as the MIC value. All equipment and culture media were sterile.

In addition to MIC, the bactericidal action of all complexes was evaluated against two Gram(+ve) and three Gram(–ve) bacteria in terms of

 © 2012 WILEY-VCH Verlag GmbH & Co. KGaA, Weinheim

Zeitschrift für anorganische und allgemeine Chemie ZAAC Journal of Inorganic and General Chemistry

colony forming unit (CFU). The inoculum for CFU of 10^6 viable bacteria per mL was prepared by diluting an overnight culture grown in LB. The bacteria were exposed to various concentrations of complexes. The final volume was 1 mL. Cultures were incubated at 37 °C for 24 h. The 100 μL bacterial culture from above was taken and spread over previously prepared agar plate and incubated for 24 h at 37 °C. The visual colonies were calculated in order to check biocidal activity of metal complexes, yielding 30–300 colonies.

4.5.2 DNA Binding Study by Absorption Titration

Hypochromism and bathochromism from intercalation mode of binding are due to strong stacking interaction between an aromatic chromophore and DNA base pair.[53,54] Selection of an appropriate absorbance peak was done by performing spectrophotometric wavelength scans of Cu^{II} complexes. After addition of equivalent amount of DNA to reference cell, both were kept for incubation of 10 min at room temperature followed by absorption measurement. It was specifically done to enable direct comparison between the assays that was required to interpret the results obtained. The intrinsic binding constant, K_b was determined by making it subject in following equation.[55]

$$[DNA]/(\varepsilon_a - \varepsilon_f) = [DNA]/(\varepsilon_b - \varepsilon_f) + 1/K_b(\varepsilon_b - \varepsilon_f)$$

where, [DNA] is the concentration of DNA in base pairs, ε_a the apparent extinction coefficient is obtained by calculating $A_{obs.}$/[complex], ε_f corresponds to the extinction coefficient of the complex in its free form and ε_b refers to the extinction coefficient of the complex in the fully bound form. When each set of data, fitted to the above equation, gave a straight line with a slope of $1/(\varepsilon_a - \varepsilon_f)$ and *y*-intercept of $1/K_b(\varepsilon_b - \varepsilon_f)$. The K_b value was determined from the ratio of the slope to intercept.

4.5.3 DNA Binding Study by Viscosity Titration

An ubbelohde viscometer immersed in a thermostatic bath maintained at 37 ± 0.1 °C was used to measure the change in hydrodynamic volume with change in complex concentration. Digital stopwatch with least count of 0.01 s was engaged for flow times measurement with accuracy of ± 0.01 s plot of $(\eta/\eta_0)^{1/3}$ vs. [complex]/[DNA] is used to study the behavior of binding, where η is the viscosity of DNA in presence of complex and η_0 is the viscosity of DNA alone. Viscosity values were calculated from the observed flow time of DNA-containing solutions (t) corrected for that of the buffer alone (t_0), $\eta = (t - t_0)$.[56]

4.5.4 DNA Cleavage Study by Gel Electrophoresis

For the gel electrophoresis experiments, total volume of 15 μL contain 300 μg·mL^{-1} of pUC19 DNA in TE buffer (10 mM Tris, 1 *mM* EDTA, pH 8.0) was treated with different complexes (200 μM) and the mixture was incubated for 24 h at 37 °C in the dark. The samples were analyzed on the base of charge and size difference on 1 % agarose gel bed consisting 0.5 μg·mL^{-1} of ethidium bromide at 50 V after quenching the reaction with 5 μL loading buffer (40 % sucrose, 0.2 % bromophenol blue). The whole bed was immersed in 1 X TAE buffer (0.04 M Tris-Acetate, pH 8, 0.001 M EDTA). Bands were visualized by UV light and photographed followed by estimating the intensity of the bands of DNA using AlphaDigiDocTM RT. Version V.4.1.0 PC-Image software; gel documentation system. The degree of DNA cleavage activity was expressed in terms of the percent of cleavage of the SC-DNA according to the following equation.[57]

4.5.5 SOD-like Activity

The NBT/NADH/PMS system was used to study SOD-like behavior of the complexes. The superoxide radial produce by 79 μM NADH, 30 μM PMS system containing 75 μM NBT, phosphate buffer (pH = 7.8), and 0.25 to 3.0 μM tested complex. The amount of reduced NBT was spectrophotometrically detected by monitoring the concentration of blue formazan form, which absorbs at 560 nm. The reduction rate of NBT was measured in presence and absence of test compounds at various concentration of complex in the system. All the measurements were carried out at room temperature. The percent inhibition (η) of NBT reduction was calculated using following equation[58]

$$\eta \text{ (percent inhibition of NBT reduction)} = (1 - k'/k) \times 100$$

where, k' and k present the slopes of the straight line of absorbance values as a function of time in presence and absence of SOD mimic or a model complex, respectively. The IC_{50} value of the complexes was determined by plotting the graph of percent inhibition of NBT reduction against increase in concentration of the complex. Concentration of the complex, which causes 50 % inhibition of NBT reduction is reported as IC_{50} (μM).

4.5.6 Cytotoxic Activity – Brine Shrimp Lethality Bioassay

Brine shrimp (*Artemia cysts*) lethality bioassay technique was applied for the determination of general toxic property of complexes. The in vitro lethality test was carried out using brine shrimp eggs i.e. *Artemia cysts*. Brine shrimp eggs were hatched in a shallow rectangular plastic dish (22 × 32 cm), filled with artificial seawater, which was prepared with commercial salt mixture and double distilled water. An unequal partition was made in the plastic dish with the help of a perforated device. Approximately 50 mg of eggs were sprinkled into the large compartment, which was darkened, while the minor compartment was opened to ordinary light. After two days nauplii were collected by a pipette from the lighter side. A stock solution of the test complex was prepared in DMSO. From this stock solution, solutions were transferred to the vials to make final concentration 2, 4, 6, 8, 10, 12 μM etc. (three for each dilutions were used for each test sample and LC_{50} is the mean of three values) and three vial was kept as control having of DMSO only. After two days, when the nauplii were ready, 1 mL of seawater and 10 of nauplii were added to each vial and the volume was adjusted with seawater to 2.5 mL per vial.[59] After 24 h each vial was observed using a magnifying glass and the number of survivors in each vial was counted and noted. Data were analyzed by simple logit method to determine the LC_{50} values, in which log of concentration of samples were plotted against percent of mortality of nauplii.[60]

Supporting Information (see footnote on the first page of this article): Material 1: Spectrophotometric titration curves and Table for equivalent endpoint determination of the complexes. Material 2: LC-MS spectrum of complex $[Cu(CPF)A^1Cl]\cdot 2H_2O$. Material 3: Thermogram of complex **1**. Material 4: CFU/mL for all complexes against different microorganisms. Material 5: Effect of complexes on brine shrimp lethality bioassay. Material 6: Physicochemical parameters of ligands A^1–A^6.

Acknowledgement

The authors thank Head, Department of Chemistry, Sardar Patel University, India for making it convenient to work in laboratory and *U.G.C.* for providing financial support under the Scheme "UGC Research Fellowship in Science for Meritorious Students".

References

[1] J. E. F. Reynolds, in: *The Extra Pharmacopeia*, 30th ed., The Pharmaceutical Press, London, **1993**, pp. 145–147.

 © 2012 WILEY-VCH Verlag GmbH & Co. KGaA, Weinheim

[2] A. S. Amin, A. A. E. Gouda, R. El-Sheikh, F. Zahran, *Spectrochim. Acta A* **2007**, *67*, 1306–1312.
[3] L. A. Mitscher, *Chem. Rev.* **2005**, *105*, 559–592.
[4] C. J. Burrows, J. G. Müller, *Chem. Rev.* **1998**, *98*, 1109–1151.
[5] I. Turel, A. Golobic, A. Klavzar, B. Pihlar, P. Buglyo, E. Tolis, D. Rehder, K. Sepcic, *J. Inorg. Biochem.* **2003**, *95*, 199–207.
[6] P. Drevensek, T. Zupancic, B. Pihlar, R. Jerala, U. Kolitsch, A. Plaper, I. Turel, *J. Inorg. Biochem.* **2005**, *99*, 432–442.
[7] I. Turel, P. Zivec, A. Pevec, S. Tempelaar, G. Psomas, *Eur. J. Inorg. Chem.* **2008**, *23*, 3718–3727.
[8] P. Drevensek, N. P. Ulrih, A. Majerle, I. Turel, *J. Inorg. Biochem.* **2006**, *100*, 1705–1713.
[9] G. Psomas, A. Tarushi, E. K. Efthimiadou, *Polyhedron* **2008**, *27*, 133–138.
[10] G. Psomas, *J. Inorg. Biochem.* **2008**, *102*, 1798–1811.
[11] D. Curman, P. Zivec, I. Leban, I. Turel, A. Polishchuk, K. D. Klika, E. Karaseva, V. Karasev, *Polyhedron* **2008**, *27*, 1489–1496.
[12] I. Turel, *Coord. Chem. Rev.* **2002**, *232*, 27–48.
[13] S. Cuzzocrea, D. P. Riley, A. P. Caputi, D. Salvemini, *Pharmacol. Rev.* **2001**, *53*, 135–159.
[14] I. Fridovich, *Science* **1978**, *201*, 875–880.
[15] M. Nagami, H. Umakoshi, T. Shimanouch, R. Kuboi, *Biochem. Eng. J.* **2004**, *21*, 221–227.
[16] A. L. Abuhijleh, C. Woods, *Inorg. Chem. Commun.* **2002**, *5*, 269–273.
[17] M. N. Patel, P. A. Parmar, D. S. Gandhi, *Bioorg. Med. Chem.* **2010**, *18*, 1227–1235.
[18] J. Mendhum, R. C. Denney, J. D. Barnes, M. J. K. Thomas, *Vogel's Text Book of Quantitative Chemical Analysis*, 6th ed., Singapore: Pearson Education PVT LTD, **2002**, 312.
[19] R. A. Day Jr., A. L. Underwood, *Quantitative Analysis*, 6th ed., Prentice-Hall of India, PVT LTD, **2006**, *388*.
[20] Z. H. Chohan, C. T. Supuran, A. Scozzafava, *J. Enzyme Inh. Med. Chem.* **2005**, *20*, 303–307.
[21] G. B. Deacon, R. Philips, *J. Coord. Chem. Rev.* **1980**, *23*, 227–250.
[22] K. Nakamoto, *Infrared and Raman Spectra of Inorganic and Coordination Compounds*, 4th ed., Wiley Interscience Publication, New York, **1986**.
[23] I. Leban, I. Turel, N. Bukovec, *J. Inorg. Biochem.* **1999**, *66*, 241–245.
[24] K. Nakamoto, *Infrared and Raman Spectra of Inorganic and Coordination Compounds*, 3rd ed., John Wiley and Sons, **1978**.
[25] M. Shebl, *J. Coord. Chem.* **2009**, *62*, 3217–3231.
[26] G. G. Mohamed, Z. H. Abd El-Wahab, *Spectrochim. Acta A* **2005**, *61*, 1059–1068.
[27] M. F. Iskander, L. EL-Sayed, N. M. H. Salem, R. W. Warner, *J. Coord. Chem.* **2005**, *58*, 125–139.
[28] G. Mendoza-Diaz, L. M. R. Martineza-Auguilera, R. Perez-Alonso, X. Solans, R. Moreno-Esparza, *Inorg. Chim. Acta* **1987**, *138*, 41–47.
[29] L. Y. Wang, Q. Y. Chen, J. Huang, K. Wang, C. J. Feng, Z. R. Gen, *Trans. Met. Chem.* **2009**, *34*, 237–245.
[30] F. A. Mautner, R. Vicente, F. R. Y. Louka, S. S. Massoud, *Inorg. Chim. Acta* **2008**, *361*, 1339–1348.
[31] R. Carballo, A. Castineiras, B. Covelo, E. Garcia-Martinez, J. Niclos, E. M. Vazquez-Lopez, *Polyhedron* **2004**, *23*, 1505–1518.
[32] B. N. Figgis, J. Lewis, in *Modern Coordination Chemistry: Principles and Methods* (Eds.: J. Lewis, R. G. Wilkins), New York, Interscience, **1960**.
[33] Q. L. Zhang, J. H. Liu, J. Z. Liu, P. X. Zhang, X. Z. Ren, Y. Liu, Y. Huang, L. N. Ji, *J. Inorg. Biochem.* **2004**, *98*, 1405–1412.
[34] C. Dendrinou-Samara, G. Psomas, C. P. Raptopoulou, D. P. Kessissoglou, *J. Inorg. Biochem.* **2001**, *83*, 7–16.
[35] G. Song, Y. He, Z. Cai, *J. Fluoresc.* **2004**, *14*, 705–710.
[36] A. M. Pyle, J. P. Rehmann, R. Meshoyrer, C. V. Kumar, N. J. Turro, J. K. Barton, *J. Am. Chem. Soc.* **1989**, *111*, 3053–3063.
[37] R. Palchaudhuri, P. J. Hergenrother, *Curr. Opin. Biotechnol.* **2007**, *18*, 497–503.
[38] A. Tarushi, C. P. Raptopoulou, V. Psycharis, A. Terzis, G. Psomas, D. P. Kessissoglou, *Bioorg. Med. Chem.* **2010**, *18*, 2678–2685.
[39] S. Ramakrishnan, M. Palaniandavar, *J. Chem. Sci.* **2005**, *117*, 179–186.
[40] J. Liu, H. Zhang, C. Chen, H. Deng, T. Lu, L. Ji, *Dalton Trans.* **2003**, 114–119.
[41] M. C. Prabahkara, H. S. Bhojya Naik, *Biometals* **2008**, *21*, 675–684.
[42] K. C. Skyrianou, F. Perdih, A. N. Papadopoulos, I. Turel, D. P. Kessissoglou, G. Psomas, *J. Inorg. Biochem.* **2011**, *105*, 1273–1285.
[43] K. C. Skyrianou, F. Perdih, I. Turel, D. P. Kessissoglou, G. Psomas, *J. Inorg. Biochem.* **2010**, *104*, 161–170.
[44] S. Sathyanarayana, J. C. Daborusak, J. B. Chaires, *Biochemistry* **1993**, *32*, 2573–2584.
[45] R. P. Hertzberg, P. B. Dervan, *J. Am. Chem. Soc.* **1982**, *104*, 312–314.
[46] R. S. Kumar, S. Arunachalam, V. S. Periasamy, C. P. Preethy, A. Riyasdeen, M. A. Akbarsha, *Eur. J. Med. Chem.* **2008**, *43*, 2082–2088.
[47] S. Sitlani, E. C. Long, A. M. Pyle, J. K. Barton, *J. Am. Chem. Soc.* **1992**, *114*, 2303–2312.
[48] J. A. Fee, in *Metal Ions in Biological Systems* (Ed.: H. Siegel), Marcel Dekker, New York, **1981**, 13.
[49] J. E. Huheey, *Inorganic Chemistry Principles of Structure and Reactivity*, 3rd ed. Harper and Row, New York, **1983**.
[50] A. M. Ramadan, M. M. EI-Naggar, *J. Inorg. Biochem.* **1996**, *63*, 143–153.
[51] F. Krohnke, *Synthesis* **1976**, *1*, 1–24.
[52] M. Alexious, I. Tsivikas, C. Dendreinou-Samara, A. A. Pantazaki, P. Trikalitis, N. Lalioti, D. A. Kyriakidis, D. P. Kessissoglou, *J. Inorg. Biochem.* **2003**, *93*, 256–264.
[53] Mudasir, N. Yoshioka, H. Inoue, *J. Inorg. Biochem.* **1999**, *77*, 239–247.
[54] A. Wolfe Jr., G. H. Shimer, T. Meehan, *Biochemistry* **1987**, *26*, 6392–6396.
[55] H. Ihmels, D. Otto, *Top. Curr. Chem.* **2005**, *258*, 161–204.
[56] S. Basili, A. Bergen, F. Dall'Acqua, A. Faccio, A. Ranzhan, H. Ihmels, S. Moro, G. Viola, *Biochemistry* **2007**, *46*, 12721–12736.
[57] J. Yang, R. N. S. Wong, M. S. Yang, *Chem. Biolog. Interact.* **2000**, *125*, 221–232.
[58] X. Le, S. Liao, X. Liu, X. Feng, *J. Coord. Chem.* **2006**, *59*, 985–995.
[59] B. N. Meyer, N. R. Ferrigni, J. E. Putnam, J. B. Jacobsen, D. E. Nicholsand, J. L. Mclaughlin, *Planta Med.* **1982**, *45*, 31–34.
[60] Md. Rafiqul Islam, S. M. Rafiqul Islam, A. S. M. Noma, J. Ara Khanam, S. M. Mohsin Ali, S. Alam, M. Woong Lee, *Mycobiology* **2007**, *35*, 25–29.

Received: February 11, 2012
Published Online: June 04, 2012

 © 2012 WILEY-VCH Verlag GmbH & Co. KGaA, Weinheim